

# Ring solids and supersolids in spherical shell-shaped dipolar Bose-Einstein condensates

J. Sánchez-Baena,<sup>1,\*</sup> R. Bombín,<sup>1,2</sup> and J. Boronat<sup>1</sup>

<sup>1</sup>*Departament de Física, Universitat Politècnica de Catalunya, Campus Nord B4-B5, 08034 Barcelona, Spain*

<sup>2</sup>*Université de Bordeaux, 351 Cours de la Libération, 33405 Talence, France*

(Dated: April 12, 2024)

We study the interplay between the anisotropy of the dipole-dipole interaction and confinement in a curved geometry by means of the extended Gross-Pitaevskii equation, which allows us to characterize the ground state of a dipolar Bose gas under the confinement of a bubble trapping potential. We do so in terms of the scattering length  $a$  and the number of particles. We observe the emergence of a wide variety of dipolar solids, consisting on arrangements of different number of droplets along a ring over the equator of the spherical shell confinement. We also show that the transition between the different phases of the system can be engineered by varying  $a$ , the number of particles or the radius of the trap, parameters which can be experimentally tuned. Finally, we show the importance of working in microgravity conditions as gravity unstabilizes the observed dipolar solids.

## I. INTRODUCTION

Since the realization of the first Bose-Einstein condensate (BEC) in 1995, the research on ultracold gases has been boosted by the achievement of a high control over them. This allows to explore not only a wide range of interaction strengths but also different geometries, ranging from one to three dimensions. In recent years, with the development of trapping techniques, it has been possible to achieve more exotic geometries with non-trivial topologies *eg.*, rings or curved surfaces (see Ref. [1] for a review on trapping techniques). These advances have motivated experiments both in zero gravity conditions [2] and with a gravity compensation mechanism [3] where the gravitational sag is absent and the BEC can be engineered in the shell of a sphere [4] (see [5] for recent reviews on the topic). Previous works include the characterization of BEC condensation and excitations [6, 7], the topological superfluid phase transition [8, 9], the BEC-BCS crossover [10], the gas to soliton transition [11], the study of vortices and collective excitations [12] and the application of matter-wave lensing techniques [13]. On a less fundamental approach, the possibility of engineering atom-based circuits has also been explored [14].

In the context of ultracold gases, the study of dipolar systems has revealed astonishing phenomena such as droplet formation and the emergence of supersolidity (see Ref. [15] for an experimental review). Supersolidity refers to a state of matter that simultaneously features spatial diagonal and off-diagonal long-range order [16–18]. In fact, dipolar systems emerge as an exceptional setup for studying the phenomena of supersolidity. This topic has been extensively studied [19–32] and experimentally confirmed [33–44]. Supersolid phases have been also predicted to occur in strictly two-dimensional geometries, where the transition to the normal state is of the Berezinskii-Kosterlitz-Thouless type [25, 26, 45, 46].

Nonetheless, only a few studies have considered this phenomena on curved surfaces (see Refs. [47–54]).

Dipolar shell-shaped systems are expected to exhibit a richer phase diagram than contact BEC gases [5]. On one hand, the long ranged and anisotropic character of dipolar interaction is known to produce density modulated phases with important long-range correlations in free space. On the other hand, the curvature would make the ground state of the system very different to that of the free space, for example by frustrating the formation of stripes. In this sense, the interplay between anisotropy, long-range order, and topology in spherically symmetric traps can give rise to BEC states in which the spherical symmetry of the trap is spontaneously broken.

To give some insight into the previously mentioned phenomena, in the present work we study a dipolar Bose gas confined on a spherical bubble trapping potential in the regime of parameters where supersolidity arises. The paper is organized as follows. In Sec. II, we illustrate the methodology that we employ. The main results of our work are presented and discussed in Sec. III. Finally, in Sec. IV we summarize the main conclusions and discuss future perspectives.

## II. THEORY

We consider a system of  $N$  magnetic dipolar atoms of mass  $m$  with all their magnetic moments  $\mu$  aligned along the  $z$ -axis. The system is confined in a bubble trap potential [55, 56]

$$V_{\text{trap}}(\mathbf{r}) = m\omega_0^2 r_0^2 \sqrt{\frac{[(r/r_0)^2 - \Delta/\epsilon]^2}{4} + (\Omega/\epsilon)^2}, \quad (1)$$

where  $\omega_0$  is the frequency of the bare harmonic trap, prior to radiofrequency (rf) dressing, and the parameters  $\Delta$  and  $\Omega$  are the detuning between the radiofrequency (rf) field and the different energy states employed to prepare the condensate, and the Rabi coupling between these states, respectively [4, 56]. We have also introduced

\* juan.sanchez.baena@upc.edu

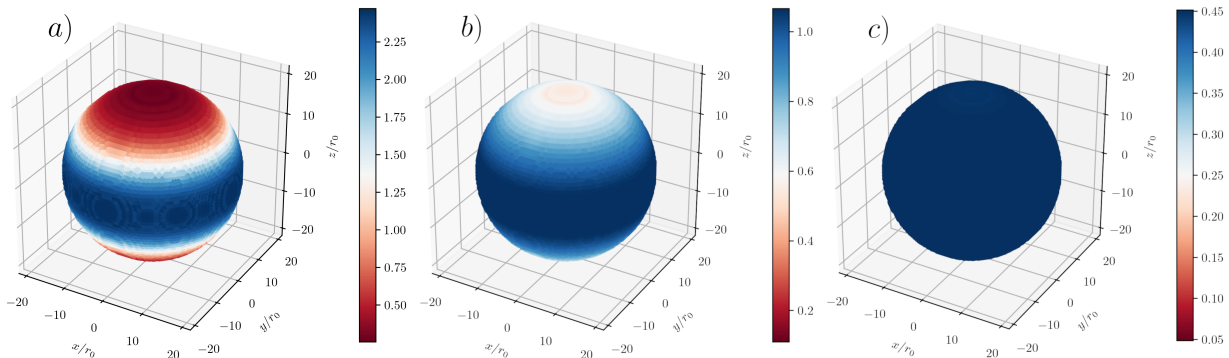


FIG. 1. Three-dimensional probability density of the dipolar BEC under a shell-shaped confinement (see Eq. 1) with detuning  $\Omega/\epsilon = \Delta/\epsilon = 400$  and bare harmonic frequency  $\omega_0 = 0.22\epsilon/\hbar$ . The probability density is reported at the surface  $r = \sqrt{x^2 + y^2 + z^2} = r_0\sqrt{\Delta/\epsilon}$  for  $\epsilon_{\text{dd}} = 1.25$  (a), 0.5 (b) and 0.1 (c). The colorbars indicate the value of  $|\Psi(\mathbf{r})|^2$  in units of  $r_0^{-3}$ .

the relevant length and energy scales,  $r_0$  and  $\epsilon$  respectively, given by  $r_0 = 12\pi a_{\text{dd}}$  and  $\epsilon = \hbar^2/(mr_0^2)$ , where  $a_{\text{dd}} = \frac{C_{\text{dd}}m}{12\pi\hbar^2}$  is the dipole length, with  $C_{\text{dd}} = \mu_0\mu^2$ ,  $\mu_0$  the Bohr magneton and  $\mu$  the magnetic dipole moment of the atoms. For simplicity, and analogously to a previous work [56], we consider  $\Delta = \Omega$ .

In order to characterize the ground state of the system in a spherically symmetric trap we solve the three-dimensional extended Gross-Pitaevskii equation that reads

$$\mu\Psi(\mathbf{r}) = \left[ -\frac{\hbar^2}{2m}\nabla^2 + V_{\text{trap}}(\mathbf{r}) + g|\Psi(r)|^2 + \gamma_{\text{QF}}|\Psi(\mathbf{r})|^3 + \int d\mathbf{r}' V_{\text{dd}}(\mathbf{r} - \mathbf{r}')|\Psi(\mathbf{r}')|^2 \right] \Psi(\mathbf{r}), \quad (2)$$

with  $\mu$  the chemical potential,  $\Psi(\mathbf{r})$  the condensate wave function, which is normalized as  $N = \int d\mathbf{r}|\Psi(\mathbf{r})|^2$ , and  $g = 4\pi\hbar^2 a_s/m$  the coupling constant with  $a_s$  the s-wave scattering length. The fourth term  $\gamma_{\text{QF}}|\Psi|^3$  is the LHY (Lee-Huang-Yang) correction [57, 58] which introduces quantum fluctuations,

$$\gamma_{\text{QF}}|\Psi|^3 = \frac{32g\sqrt{a_s^3}}{3\sqrt{\pi}} Q_5(\epsilon_{\text{dd}}) |\Psi|^3, \quad (3)$$

with  $\epsilon_{\text{dd}} = a_{\text{dd}}/a_s$  and  $Q_5(\epsilon_{\text{dd}}) = \frac{1}{2} \int_0^\pi d\alpha \sin\alpha [1 + \epsilon_{\text{dd}}(3\cos^2\alpha - 1)]^{5/2}$ . Finally, the last term in Eq. (2) accounts for the dipole-dipole interaction (DDI),

$$V_{\text{dd}}(\mathbf{r} - \mathbf{r}') = \frac{C_{\text{dd}}}{4\pi} \frac{1 - 3\cos^2\theta}{|\mathbf{r} - \mathbf{r}'|^3}, \quad (4)$$

where  $\theta$  is the polar angle of the vector  $\mathbf{r} - \mathbf{r}'$ .

The use of the pseudopotential in Eq. 2 (that is, the term  $g|\Psi(r)|^2 + \int d\mathbf{r}' V_{\text{dd}}(\mathbf{r} - \mathbf{r}')|\Psi(\mathbf{r}')|^2$ ) is justified as long as the collisions between particles can be treated as three-dimensional processes. The system lays in the two dimensional regime if the harmonic length  $a_{\text{ho}} = \sqrt{\hbar/(m\omega_0)}$ ,

which is associated to the tightness of the confinement, is significantly smaller than any other length scales. However, in our calculations, we choose a trapping strength such that  $a_{\text{ho}} \gg a_s$ . Therefore, all scattering processes can be considered three-dimensional and the pseudopotential of Eq. 2 can be applied. In the case of a tight confinement (thin shell limit), a pseudopotential that considers the effects of the geometry should be employed [59, 60].

In the majority of this work, we restrict ourselves to the zero gravity limit. However, the effect of a gravitational force can be accounted for by adding the following one-body potential [49] to Eq. 2

$$V_g(\mathbf{r}) = mg(x \sin\theta_g + z \cos\theta_g), \quad (5)$$

where  $\theta_g$  is the angle between the  $z$ -axis and the gravity direction. For  $^{164}\text{Dy}$  atoms, the gravitational strength on the Earth corresponds to  $mg = 1.15\epsilon/r_0 = mg_E$ . In Sec. III D, we study the robustness of a dipolar solid ring under the effect of gravity.

### III. RING SOLIDS AND SUPERSOLIDS

As a means to illustrate the system under study, we show in Fig. 1 the probability density of the dipolar BEC confined within the bubble trap under zero gravity for different values of the ratio  $\epsilon_{\text{dd}} = a_{\text{dd}}/a_s$ . We have employed a trap with parameters  $\Delta/\epsilon = 400$ ,  $\omega_0 = 0.22\epsilon/\hbar$ , which correspond to  $\omega_0 = 2\pi \times 200$  Hz and a bubble trap with radius  $R = r_0\sqrt{\Delta/\epsilon} = 5.2 \mu\text{m}$  for  $^{164}\text{Dy}$  atoms. These parameters are realistic for a setting with non-dipolar gases. From the figure, we can see that in the contact dominated regime ( $\epsilon_{\text{dd}} \ll 1$ ), the dipolar gas fills up the spherical shell, yielding an apparently spherically symmetric density distribution, despite the anisotropy of the DDI. As seen in Fig. 1, and as reported in previous works [48, 49], the atoms of the BEC gas tend to populate the equator of the shell, even before reaching

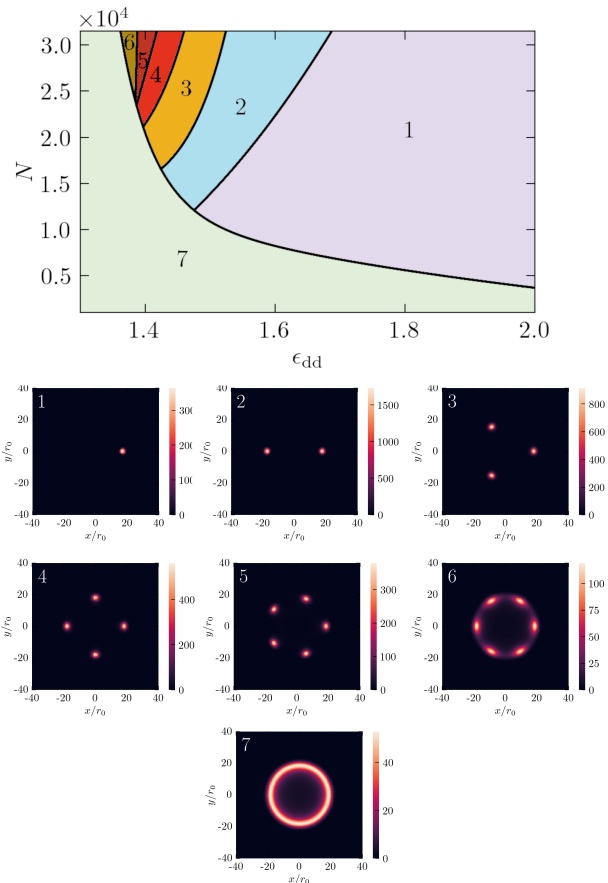


FIG. 2. Top: structural diagram of the ring-shaped dipolar condensate as a function of  $\epsilon_{\text{dd}} = a_{\text{dd}}/a$  and the number of particles  $N$ . Panels 1-7: integrated density profiles  $\rho(x, y)$  of the condensate density arising in each region of the diagram. The colorbars indicate the value of  $\rho(x, y)$  in units of  $r_0^{-2}$ . The parameters for the bubble trap (see Eq. 1) are  $\Delta/\epsilon = \Omega/\epsilon = 400$ ,  $\omega_0 = 0.22\epsilon/\hbar$ .

the dipole dominated regime,  $\epsilon_{\text{dd}} > 1$ . This magnetostriction is a consequence of the competition between the anisotropy of the dipole-dipole interaction (which energetically favours head-to-tail arrangements of dipoles) and the shell shape of the external confinement. Experimentally, ring shaped condensates can be obtained by the use of toroidal traps [50, 61–63], which can also be realized in experiments [64–66]. However, in the present case, as well as for cylindrically-shaped traps [67], the ring shape of the condensate arises purely due to magnetostriction in a spontaneous manner, instead of being entirely forced by the external confinement. For the rest of our work, we focus on the regime  $\epsilon_{\text{dd}} > 1$  and the aforementioned value of the trapping strength.

In the dipolar dominated regime ( $\epsilon_{\text{dd}} > 1$ ), the anisotropy of the dipolar interaction can give rise to dipolar solids and supersolids, in analogy to the phenomenology that takes place in bulk-trapped dipolar BECs. Eq. 2 can numerically be solved for different values of the scat-

tering length  $a_s$  (and thus,  $\epsilon_{\text{dd}}$ ) and number of particles  $N$  to obtain the ground state of the system. As reported in similar works [62, 68, 69], the energy minimization has to be carefully performed, sampling a wide variety of initial conditions, as many metastable states close to the ground state exist. We detail in the Appendix A the numerical parameters of our simulations, as well as the initial conditions considered. Since superfluid structures may arise, we evaluate the Leggett’s upper bound estimator for superfluidity [70], which is computed from the ground state density as

$$f_s = \left[ \frac{1}{2\pi} \int_0^{2\pi} \frac{d\theta}{\rho(\theta)/\rho_0} \right]^{-1}, \quad (6)$$

where

$$\rho(\theta) = \int dz dr r |\Psi(r, \theta, z)|^2, \quad (7)$$

$$\rho_0 = \frac{1}{2\pi} \int_0^{2\pi} \rho(\theta) d\theta. \quad (8)$$

Eq. 6 yields the trivial unity limit for a ring-like condensate (since  $\rho(\theta)$  is a constant) and decreases as the modulation of the wave function increases along the ring. This upper-bound estimator for the superfluidity has shown excellent agreement with the calculation of non-classical translational inertia for a system of dipoles confined in a quasi-1D tubular geometry [31].

### A. Structural diagram and transitions

The structural diagram of the system is reported in Fig. 2, where we show the two-dimensional integrated density  $\rho(x, y) = \int dz |\Psi(\mathbf{r})|^2$  of each structure. Regarding the superfluid fraction along the ring, only the structures featuring dipolar clusters in the interval  $\epsilon_{\text{dd}} \in (1.36, 1.41)$  yield a significant superfluidity ( $f_s > 0.2$ ), while for  $\epsilon_{\text{dd}} > 1.41$ , the result of Eq. 6 quickly drops to zero. On the other hand, all the states in the SF region of Fig. 2 yield unit superfluidity. We label the states with  $f_s = 1$  as superfluids, while we call supersolids and solids those which yield  $f_s > 0.2$  and  $f_s < 0.2$ , respectively. In general, the increase of  $\epsilon_{\text{dd}}$  for a fixed number of particles implies a lower number of droplets, since the attraction of the DDI favours the bunching of dipoles and thus, fewer and more elongated clusters are formed. In much the same way, the decrease of the number of particles for a fixed  $\epsilon_{\text{dd}}$  also causes a reduction in the number of droplets because the system wants to maximize the number of dipoles placed in a head-to-tail configuration. The peak density of the droplets that we obtain lies close to the expected values obtainable with harmonic traps (see the seminal experiment of Ref. [71]). For the largest number of particles ( $N = 31500$ ) the peak density lies in the interval  $\rho_{\text{peak}} \in [3, 100] \times 10^{14} \text{ cm}^{-3}$ , where the largest values are achieved for  $\epsilon_{\text{dd}} = 2$ , for which all particles cluster into a single droplet. We also see that

the solid structures disappear if the number of particles is decreased below a threshold, from which there is not enough density to sustain clustering. This phenomenology is reminiscent of a quasi-1D system of dipoles confined in a tube [30, 31] where the disappearance of the supersolid phase in the low density regime upon decreasing the density is also reported.

Precisely, in the spirit of these works, it is interesting to examine the character (continuous or discontinuous) of the transition between the different structures present in the diagram of Fig. 2. We can not strictly speak of first and second order phase transitions (as it is done in [30, 31]) because our system is finite. Our calculations show that the transition between different solid states is discontinuous, meaning that the system jumps from a state with a given number of droplets to a different one discontinuously (the density distribution changes abruptly). This is because there exists an energy crossing between the different metastable states at the transition boundary. We illustrate this in Fig. 3, where we report the energy difference between two dipolar solids across the transition between regions 3 and 4 of the diagram in Fig. 2 for  $N = 31500$ . In much the same way, the transition between a dipolar solid and the superfluid is also discontinuous, in analogy to the first order phase transition that takes place in the low density regime of the tubular quasi-1D system. This is illustrated in Fig. 4, where we show the contrast of the BEC density across the transition between regions 2 and 7 of Fig. 2, for  $N = 16500$ . Here, the contrast is defined as

$$C = \frac{\rho_{\max.} - \rho_{\min.}}{\rho_{\max.} + \rho_{\min.}} \quad (9)$$

where  $\rho_{\max.}$  and  $\rho_{\min.}$  are, respectively, the maximum and minimum values of the integrated density  $\rho(x, y)$  along the circle of radius  $R/r_0 = \sqrt{\Delta/\epsilon}$ . As one can see from Fig. 4, the contrast in the density shows a clear discontinuity. Therefore, in view of the results, we can draw similarities between the physics under our geometry and the quasi-1D tubular one, since the transition that leads to a superfluid gas in our system is analogous to the first-order phase transition of Refs. [30, 31].

### B. Engineering supersolids

Even though the supersolid phase constitutes a small region in the diagram of Fig. 2 as mentioned previously, a rich variety of supersolid structures can be engineered when tuning  $\Delta$ , and thus effectively modifying the radius of the trapping spherical shell. By increasing  $\Delta$  starting from a conventional harmonically trap gas, the system transitions to a supersolid. Further increasing  $\Delta$  leads to an increase in the number of droplets, all while retaining a substantial superfluid fraction and the ring shape. This is shown in Fig. 5, where we report the integrated density  $\rho(x, y)$  of the condensate wave function for different values of  $\Delta$ . We also report Leggett's upper bound for

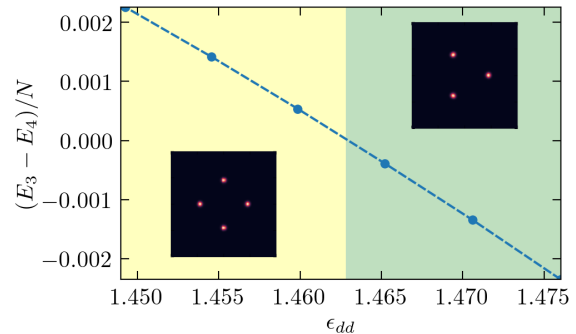


FIG. 3. Difference in the energy per particle between a solid state with 3 and 4 droplets as a function of  $\epsilon_{dd}$  for  $N = 31500$  and the same bubble trap as in Fig. 2.

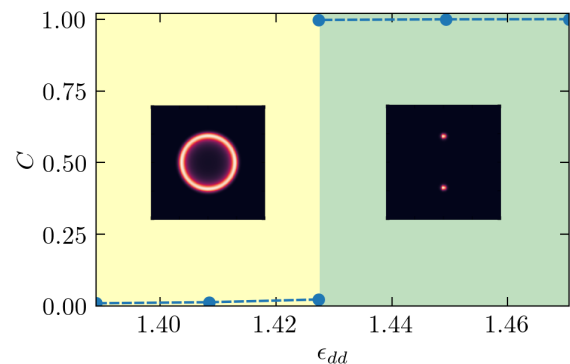


FIG. 4. Contrast of the BEC density (see Eq. 9) as a function of  $\epsilon_{dd}$  for  $N = 16500$ . The bubble trap parameters are the same as in Fig. 2.

the superfluid fraction (see Eq. 6), which increases as the trap radius decreases, thus confirming that the superfluid density can be enhanced by reducing  $\Delta$ . The variation of this parameter is pretty straightforward in experimental setups, as changing  $\Delta$  is precisely how the bubble trap is generated from a harmonic potential. The wide variety of solid structures in the diagram of Fig. 2 thus allows for the observation of many different supersolid dipolar rings (i.e. supersolids with a different number of droplets) by playing with the parameter  $\Delta$  starting from different points of the structural diagram. This is showcased in Fig. 6, where we show four examples of different supersolids obtained for different combinations of the number of particles, the detuning and the scattering length.

### C. High particle number limit

Up to now, we have restricted the particle number to the interval  $N \leq 31500$ . However, it is interesting to consider higher particle numbers, specifically to check whether a secondary, or even multiple rings can arise. In order to address this question, we have computed

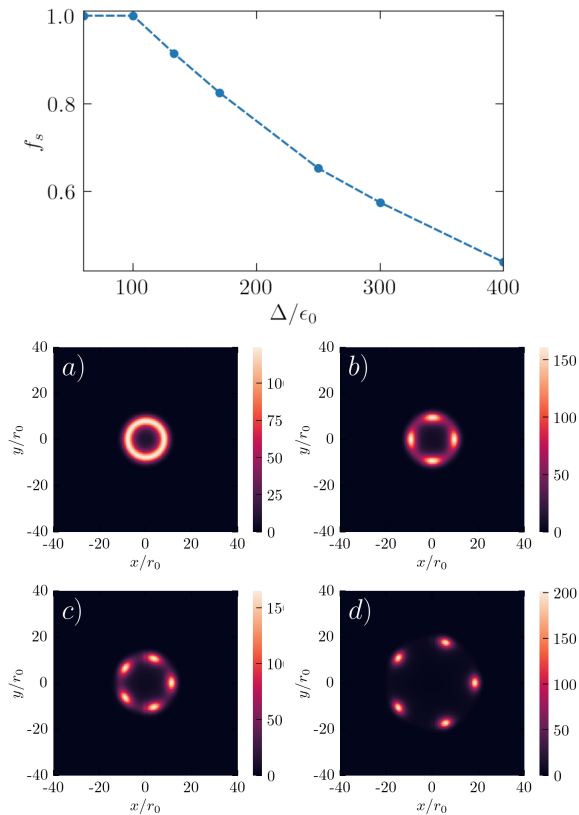


FIG. 5. *Top*: Superfluid density as a function of the detuning  $\Delta/\epsilon$ . *Bottom*: Integrated density  $\rho(x, y)$  for detuning values  $\Delta/\epsilon = 100, 133, 170$ , and  $400$  from a) to d), respectively. The colorbars indicate the value of  $\rho(x, y)$  in units of  $r_0^{-2}$ . The ratio between the dipole length and the scattering length is set to  $\epsilon_{\text{dd}} = 1.38$  and  $N = 26500$ . The bare harmonic frequency is the same as in Fig. 2.

the ground state of the dipolar BEC for  $N = 10^5$  and  $N = 10^6$  for two different values of  $\epsilon_{\text{dd}}$  ( $\epsilon_{\text{dd}} = 1.42$  and  $\epsilon_{\text{dd}} = 1.72$ ). For these cases, we show in Fig. 7 the integrated two-dimensional densities  $\rho(x, y) = \int dz |\Psi(\mathbf{r})|^2$  and  $\rho(x, z) = \int dy |\Psi(\mathbf{r})|^2$ . As we can see from the figure, atoms accumulate on the central ring instead of forming additional ones, which gets wider as the number of particles increases. Looking at the case with  $\epsilon_{\text{dd}} = 1.72$ , one can also see that increasing the number of particles leads the system to an unstructured superfluid, meaning that there exists an upper threshold for the particle number above which the solid and supersolid structures disappear. Again, this is in line to the phenomenology reported in the quasi-1D tubular geometry, where in the high density region of the phase diagram, increasing the density drives a supersolid-to-superfluid phase transition [30, 31].

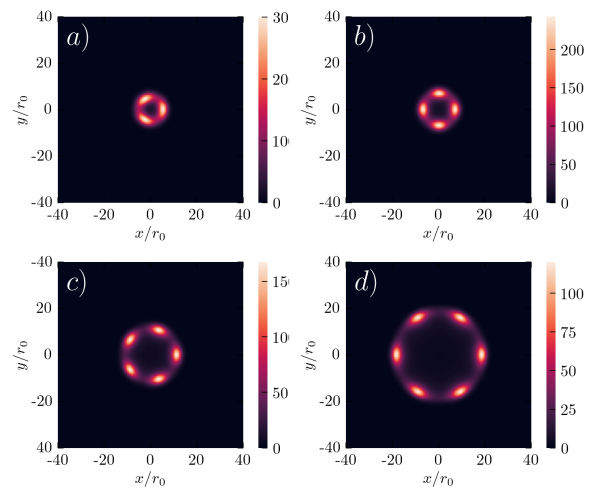


FIG. 6. Ring shaped supersolid dipolar states are engineered by appropriate combinations of values of the magnetic field detuning, the scattering length and the number of particles. Panels a)-d) show the integrated density  $\rho(x, y)$  of supersolid states obtained for  $\epsilon_{\text{dd}} = 1.43$ ,  $N = 26500$ ,  $\Delta/\epsilon = 50$  (a),  $\epsilon_{\text{dd}} = 1.41$ ,  $N = 26500$ ,  $\Delta/\epsilon = 80$  (b),  $\epsilon_{\text{dd}} = 1.39$ ,  $N = 26500$ ,  $\Delta/\epsilon = 170$  (c),  $\epsilon_{\text{dd}} = 1.37$ ,  $N = 31500$ ,  $\Delta/\epsilon = 400$  (d). The colorbars indicate the value of  $\rho(x, y)$  in units of  $r_0^{-2}$ . The bare harmonic frequency is the same as in Fig. 2.

#### D. Effect of gravity

The structural diagram reported in Fig. 2 has been computed assuming zero gravity conditions. Experimentally, and as stated before, microgravity conditions are achievable in the NASA Cold Atom laboratory in the International Space Station. However, it is interesting to explore the effect of a gravitational force on the dipolar arrangements that have been reported, to study how robust these structures are with respect to gravity. We account for gravitational effects through the inclusion of the one-body potential of Eq. 5. We have performed calculations for  $\epsilon_{\text{dd}} = 1.47$ ,  $N = 31500$  (which yields a solid state with 3 droplets in the absence of gravity) varying the strength of the gravitational field. We first consider a gravity vector with  $\theta_g = 0$ . The results are shown in Fig. 8. For values of the gravity strength  $mg < 0.03mg_E$ , the structure of the dipolar BEC is not significantly altered, while for  $mg > 0.04mg_E$  we observe the melting of the solid configuration into a superfluid, clusterless state. This indicates that, for these parameters, the gravitational force field of the Earth would destroy the solid arrangement of droplets, in contrast to what happens in the different parameter regime considered in Ref. [48]. This is because our calculations do not lie in the thin-shell limit considered in Ref. [48], since a tighter trap confinement implies a higher energy cost for particles to accumulate in a reduced space at the bottom of the trap. We have also performed calculations changing the relative orientation between the gravity field and the  $z$ -axis to  $\theta_g = \pi/4$ . We show the results in Fig. 9. In this

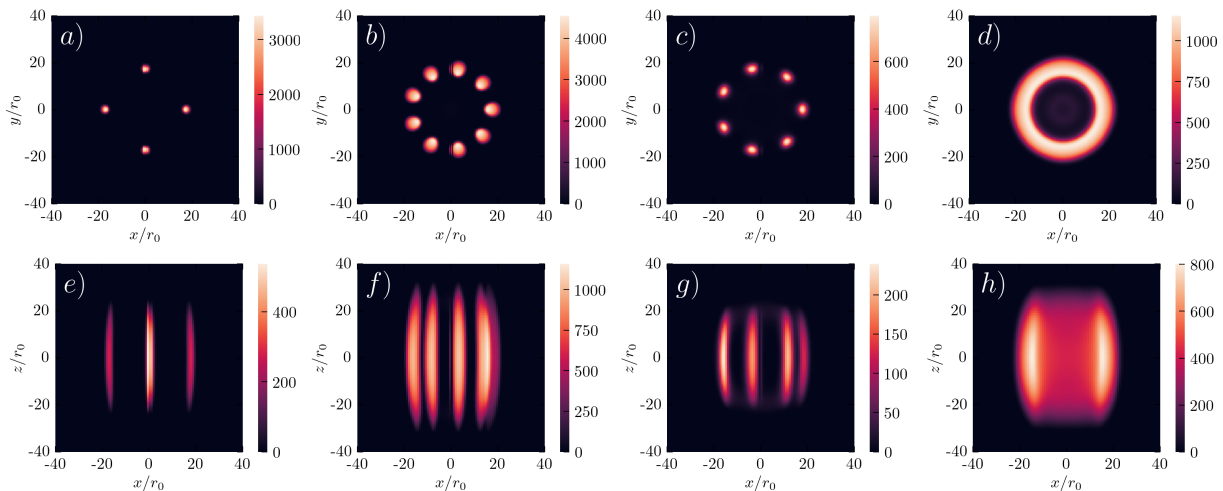


FIG. 7. Integrated densities  $\rho(x, y)$  (top) and  $\rho(x, z)$  (bottom) for  $\varepsilon_{\text{dd}} = 1.72$ ,  $N = 10^5$  ((a), (e)),  $\varepsilon_{\text{dd}} = 1.72$ ,  $N = 10^6$  ((b), (f)),  $\varepsilon_{\text{dd}} = 1.42$ ,  $N = 10^5$  ((c), (g)) and  $\varepsilon_{\text{dd}} = 1.42$ ,  $N = 10^6$  ((d), (h)). The bubble trap parameters are the same as in Fig. 2. The colorbars indicate the value of  $\rho(x, y)$  and  $\rho(x, z)$  in units of  $r_0^{-2}$ .

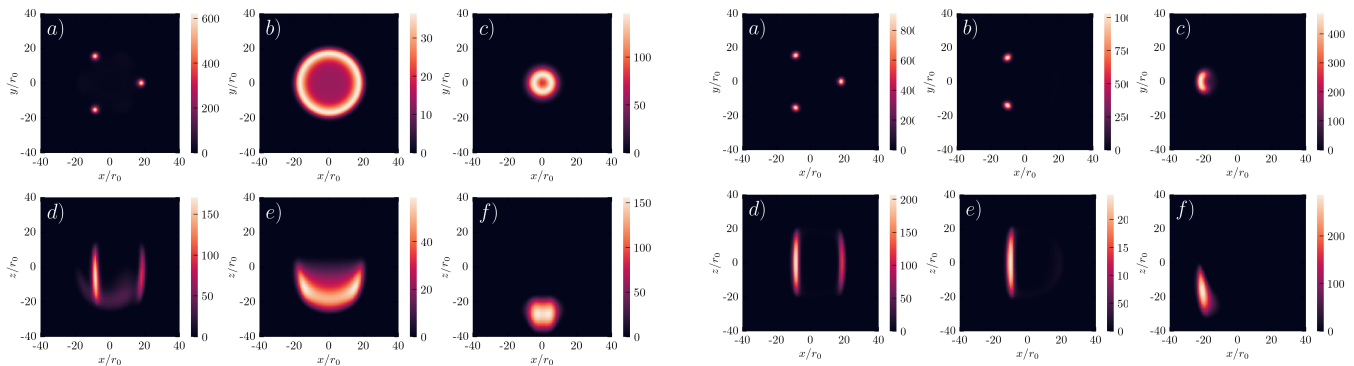


FIG. 8. Integrated densities  $\rho(x, y)$  ((a)-(c)) and  $\rho(x, z)$  ((d)-(f)) for a varying gravitational strength  $mg = 0.03mg_E$  ((a), (d)),  $mg = 0.04mg_E$  ((b), (e)) and  $mg = 0.5mg_E$  ((c), (f)) and an angle  $\theta_g = 0$  (see Eq. 5). The bubble trap parameters are the same as in Fig. 2. The colorbars indicate the value of  $\rho(x, y)$  and  $\rho(x, z)$  in units of  $r_0^{-2}$ .

case, we find that the three droplet structure remains unaltered up to  $mg \simeq 0.0025mg_E$ , where gravity induces a transition into a two droplet state. Further increasing the gravitational strength leads to the merging of the two dipolar clusters into one.

### E. Comparison with previous works

Previous works have explored the formation of supersolid structures in curved trapping geometries. Authors in Ref. [48] also explore the supersolid properties on dipolar BECs confined in a bubbled trap. However, they do so through the use of an ab-initio Monte Carlo method. In comparison to the results from Fig. 2, their results involve a considerably lower number of particles ( $N < 300$ ),

FIG. 9. Integrated densities  $\rho(x, y)$  ((a)-(c)) and  $\rho(x, z)$  ((d)-(f)) for a varying gravitational strength  $mg = 0.0001mg_E$  ((a), (d)),  $mg = 0.0025mg_E$  ((b), (e)) and  $mg = 0.5mg_E$  ((c), (f)) and an angle  $\theta_g = \pi/4$  (see Eq. 5). The bubble trap parameters are the same as in Fig. 2. The colorbars indicate the value of  $\rho(x, y)$  and  $\rho(x, z)$  in units of  $r_0^{-2}$ .

a shell of smaller radius, and lie in the thin-shell limit, where Eq. 2 is no longer valid, and a pseudopotential that accounts for the curvature of the confinement has to be applied. Ref. [48] shows supersolid and solid structures with four dipolar clusters along the equator of the sphere, much like the structure that emerges in region 4 of the structural diagram of Fig. 2. The physics of dipolar BECs under a bubble trap has also been studied in Ref. [54]. In comparison to our work, they employ a higher number of particles ( $N = 60000$ ), a considerably higher trap radius  $R = 21\mu\text{m}$  and a detuning not equal to the Rabi coupling,  $\Delta \neq \Omega$ , which favours the emergence of a higher number of dipolar clusters compared to the structures reported in our Fig. 2. Remarkably, it is reported that supersolidity can be induced in solid arrangements of dipolar clusters by inducing a rotation

in the system [54]. Other works have considered different kind of curved geometries, like toroidal traps [50, 62] and box traps [67]. Toroidal traps produce ring shaped supersolids analogous to the ones found in this work, the difference being that under a shell-shaped confinement, and under microgravity conditions, the ring shape of the supersolid arises naturally from magnetostriction, instead of being imposed by the trapping confinement. In Ref. [62], the transition between a fluid ring into a supersolid, with 8 dipolar droplets as  $\epsilon_{dd}$  increases, is reported. The authors employ a toroidal trap with a considerably higher trapping strength of  $\omega = 2\pi \times 1000$  Hz compared to our parameters, which explains the higher number of clusters that they observe compared to our results, since a higher trapping confinement limits the length of the droplets along the polarization direction and hence forces the system to organize in a higher number of clusters. On the other hand, the physics of anti-dipolar BECs have been recently addressed in toroidal traps [53], where the formation of stacks of ring-shaped droplets, which can coherently overlap to form a supersolid, has been reported. In regards to results in a box potential, Ref. [67] explores different shapes for the box confinement, including a cylindrically shaped box trap, where ring solids and supersolids arise. Compared to our work, the authors in Ref. [67] consider a larger number of atoms, which induces the emergence of a larger number of droplets.

#### IV. CONCLUSIONS

We have studied the interplay between the anisotropy of the dipole-dipole interaction and the curved geometry of the trapping potential for a dipolar condensate confined in a bubble trap. We have provided the structural diagram of a dipolar BEC as a function of the number of particles  $N$  and the ratio between the dipole length and the scattering length  $\epsilon_{dd}$ , and have reported the emergence of a wide variety of ring shaped solid structures formed by arrangements of dipolar clusters along the equator of the trapping potential. We have characterized the transitions between different structures, showing that they are discontinuous, reminiscent of a first order phase transition in the thermodynamic limit. This establishes a clear connection between our system and a dipolar BEC trapped in a quasi-1D configuration, where, in the low density regime, a first-order phase transition between a superfluid and a solid phase takes place. We have also explored the high particle number limit ( $N > 10^5$ ) and have observed that atoms accumulate in the central ring along the equator of the trap instead of forming secondary ring-like structures. We have shown that supersolid states with varying number of dipolar clusters can be engineered by changing  $N$ ,  $\epsilon_{dd}$ , and the effective radius of the trap, which is accomplished by tuning the detuning of the coupled rf field. In regards to the robustness of the dipolar structures, we have also considered the

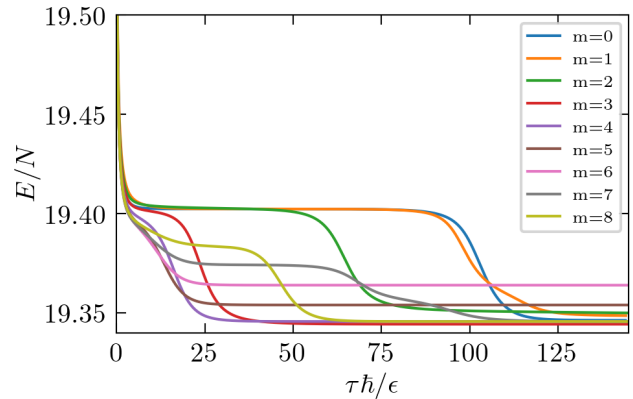


FIG. 10. Energy per particle as a function of the imaginary time for the different initial conditions given by Eq. A1. The parameters are  $\epsilon_{dd} = 1.47$ ,  $N = 31500$ ,  $\Delta/\epsilon = 400$

effect of a gravitational field and have shown that, for our parameters of choice, the gravitational field of the Earth would destroy an arrangement of dipolar droplets, forcing particles to accumulate at the bottom of the trap. Our results lead to the existence of ring shaped dipolar supersolid states with varying number of clusters which, unlike in the case of ring-shaped traps, are not entirely forced by the confinement geometry, and arise instead as a result of the competition between the anisotropy of the DDI and the shell-shaped geometry of the bubble trap.

The study of the excitations of these ring supersolids remains a relevant question to be addressed, since it could lead to an experimental protocol to probe the gas-to-supersolid transition by means of measuring excitation frequencies. Also, it remains an open question how finite temperature could affect the physics of the dipolar system under these trapping conditions. Recent results [32, 72, 73] reveal an important impact of thermal fluctuations on dipolar gases, leading to the counterintuitive formation of a supersolid by heating in the ultracold regime.

#### ACKNOWLEDGMENTS

We acknowledge financial support from Ministerio de Ciencia e Innovación MCIN/AEI/10.13039/501100011033 (Spain) under Grant No. PID2020-113565GB-C21 and from AGAUR-Generalitat de Catalunya Grant No. 2021-SGR-01411. J.S.B and R.B acknowledge European Union-NextGenerationEU, Ministry of Universities and Recovery, Transformation and Resilience Plan, through a call from the Technical University of Catalonia. R.B. further acknowledges funding from the European Union's Horizon 2020 research and innovation programme under the Marie Skłodowska-Curie Grant Agreement No. 101034379.

## Appendix A: Numerical implementation

All the results shown in this work are obtained by propagating Eq. 2 in imaginary time. To do so, we discretize space and work with a grid of  $(N_x, N_y, N_z) = (200, 200, 100)$  points, in a simulation box of size  $(L_x/r_0, L_y/r_0, L_z/r_0) = (80, 80, 80)$ . During imaginary time propagation, we employ a time step of  $d\tau\hbar/\epsilon = 0.0005$ . The DDI term of Eq. 2 is evaluated by computing its Fourier transform through an FFT routine. As mentioned in the main text, during the imaginary time evolution of Eq. 2 it is very likely for the system to get stuck in a metastable state. Because of this, we set multiple calculations starting from a variety of initial conditions when computing the ground state of the system for a given set of values  $(N, \epsilon_{\text{dd}}, \Delta/\epsilon)$ . The set of initial

conditions employed is given by

$$\Psi_0(\mathbf{r}) = \exp\left(-\frac{\omega_0\hbar}{\epsilon}\left(r/r_0 - \sqrt{\Delta/\epsilon}\right)^2\right) \times (1 + 0.5 \cos(m\phi)) \quad (\text{A1})$$

where  $r = |\mathbf{r}|$ ,  $\phi$  is the azimuthal angle and  $m = 0, 1, 2, \dots, 8$ . This allows us to start from initial configurations close in shape to those with  $m$  number of clusters. After imaginary time evolution, we retain the state with the lowest energy as the ground state. In order to illustrate this process, and to showcase the rich metastable landscape of the system, we show in Fig. 10 the energy as a function of the imaginary time for the different initial states for  $\epsilon_{\text{dd}} = 1.47$ ,  $N = 31500$ ,  $\Delta/\epsilon = 400$ .

- 
- [1] Barry M Garraway and H el ene Perrin, “Recent developments in trapping and manipulation of atoms with adiabatic potentials,” *Journal of Physics B: Atomic, Molecular and Optical Physics* **49**, 172001 (2016).
- [2] Dennis Becker, Maik D. Lachmann, Stephan T. Seidel, Holger Ahlers, Aline N. Dinkelaker, Jens Grosse, Ortwin Hellmig, Hauke M untzinga, Vladimir Schkolnik, Thijs Wendrich, Andr e Wenzlawski, Benjamin Weps, Robin Corgier, Tobias Franz, Naceur Gaaloul, Waldemar Herr, Daniel L udtke, Manuel Popp, Sirine Amri, Hannes Duncker, Maik Erbe, Anja Kohfeldt, Andr e Kubelka-Lange, Claus Braxmaier, Eric Charron, Wolfgang Ertmer, Markus Krutzik, Claus L ammerzahl, Achim Peters, Wolfgang P. Schleich, Klaus Sengstock, Reinhold Walser, Andreas Wicht, Patrick Windpassinger, and Ernst M. Rasel, “Space-borne bose–einstein condensation for precision interferometry,” *Nature* **562**, 391–395 (2018).
- [3] Yanliang Guo, Emmanuel Mercado Gutierrez, David Rey, Thomas Badr, Aur elien Perrin, Laurent Longchambon, Vanderlei Salvador Bagnato, H el ene Perrin, and Romain Dubessy, “Expansion of a quantum gas in a shell trap,” *New Journal of Physics* **24**, 093040 (2022).
- [4] R. A. Carollo, D. C. Aveline, B. Rhyno, S. Vishveshwara, C. Lannert, J. D. Murphree, E. R. Elliott, J. R. Williams, R. J. Thompson, and N. Lundblad, “Observation of ultracold atomic bubbles in orbital microgravity,” *Nature* **606**, 281–286 (2022).
- [5] A. Tononi and L. Salasnich, “Shell-shaped atomic gases,” (2023), arXiv:2309.15710 [cond-mat.quant-gas].
- [6] Nat alia S M oller, F Ednilson A dos Santos, Vanderlei S Bagnato, and Axel Pelster, “Bose–einstein condensation on curved manifolds,” *New Journal of Physics* **22**, 063059 (2020).
- [7] A. Tononi, F. Cinti, and L. Salasnich, “Quantum bubbles in microgravity,” *Phys. Rev. Lett.* **125**, 010402 (2020).
- [8] A. Tononi and L. Salasnich, “Bose–einstein condensation on the surface of a sphere,” *Phys. Rev. Lett.* **123**, 160403 (2019).
- [9] Andrea Tononi, Axel Pelster, and Luca Salasnich, “Topological superfluid transition in bubble-trapped condensates,” *Phys. Rev. Res.* **4**, 013122 (2022).
- [10] Yan He, Hao Guo, and Chih-Chun Chien, “Bcs-bec crossover of atomic fermi superfluid in a spherical bubble trap,” *Phys. Rev. A* **105**, 033324 (2022).
- [11] A. Tononi, G. Astrakharchik, and D. S. Petrov, “Gas-to-soliton transition of attractive bosons on a spherical surface,” (2023), arXiv:2312.04984 [cond-mat.quant-gas].
- [12] Andrea Tononi and Luca Salasnich, “Low-dimensional quantum gases in curved geometries,” *Nature Reviews Physics* **5**, 398–406 (2023).
- [13] Patrick Boegel, Alexander Wolf, Matthias Meister, and Maxim A Efremov, “Controlled expansion of shell-shaped bose–einstein condensates,” *Quantum Science and Technology* **8**, 034001 (2023).
- [14] Luigi Amico, Dana Anderson, Malcolm Boshier, Jean-Philippe Brantut, Leong-Chuan Kwek, Anna Minguzzi, and Wolf von Klitzing, “Colloquium: Atomtronic circuits: From many-body physics to quantum technologies,” *Rev. Mod. Phys.* **94**, 041001 (2022).
- [15] Lauriane Chomaz, Igor Ferrier-Barbut, Francesca Ferlaino, Bruno Laburthe-Tolra, Benjamin L Lev, and Tilman Pfau, “Dipolar physics: a review of experiments with magnetic quantum gases,” *Reports on Progress in Physics* **86**, 026401 (2022).
- [16] A. F Andreev and I. M. Lifshitz, “Quantum theory of defects in crystals,” *Sov. Phys. JETP* **29**, 1107–1113 (1969).
- [17] G. V. Chester, “Speculations on bose–einstein condensation and quantum crystals,” *Phys. Rev. A* **2**, 256–258 (1970).
- [18] A. J. Leggett, “Can a solid be “superfluid”?” *Phys. Rev. Lett.* **25**, 1543–1546 (1970).
- [19] Fabian B ottcher, Jan-Niklas Schmidt, Jens Hertkorn, Kevin S H Ng, Sean D Graham, Mingyang Guo, Tim Langen, and Tilman Pfau, “New states of matter with fine-tuned interactions: quantum droplets and dipolar supersolids,” *Reports on Progress in Physics* **84**, 012403 (2020).
- [20] Tobias Ilg and Hans Peter B uchler, “Ground-state stability and excitation spectrum of a one-dimensional dipolar supersolid,” *Phys. Rev. A* **107**, 013314 (2023).
- [21] J. Hertkorn, J.-N. Schmidt, M. Guo, F. B ottcher, K. S. H. Ng, S. D. Graham, P. Uerlings, T. Langen, M. Zwierlein, and T. Pfau, “Pattern formation in quantum ferrofluids:



- From supersolids to superglasses,” *Phys. Rev. Res.* **3**, 033125 (2021).
- [22] Albert Gallemí and Luis Santos, “Superfluid properties of a honeycomb dipolar supersolid,” *Phys. Rev. A* **106**, 063301 (2022).
- [23] J. Hertkorn, J.-N. Schmidt, M. Guo, F. Böttcher, K. S. H. Ng, S. D. Graham, P. Uerlings, H. P. Büchler, T. Langen, M. Zwierlein, and T. Pfau, “Supersolidity in two-dimensional trapped dipolar droplet arrays,” *Phys. Rev. Lett.* **127**, 155301 (2021).
- [24] P Blair Blakie, D Baillie, and Sukla Pal, “Variational theory for the ground state and collective excitations of an elongated dipolar condensate,” *Communications in Theoretical Physics* **72**, 085501 (2020).
- [25] R. Bombín, J. Boronat, and F. Mazzanti, “Dipolar bose supersolid stripes,” *Phys. Rev. Lett.* **119**, 250402 (2017).
- [26] Raúl Bombín, Ferran Mazzanti, and Jordi Boronat, “Berezinskii-kosterlitz-thouless transition in two-dimensional dipolar stripes,” *Phys. Rev. A* **100**, 063614 (2019).
- [27] Yong-Chang Zhang, Fabian Maucher, and Thomas Pohl, “Supersolidity around a critical point in dipolar bose-einstein condensates,” *Phys. Rev. Lett.* **123**, 015301 (2019).
- [28] Yong-Chang Zhang, Thomas Pohl, and Fabian Maucher, “Phases of supersolids in confined dipolar bose-einstein condensates,” *Phys. Rev. A* **104**, 013310 (2021).
- [29] Yong-Chang Zhang, Thomas Pohl, and Fabian Maucher, “Metastable patterns in one- and two-component dipolar bose-einstein condensates,” (2023), arXiv:2310.04738 [cond-mat.quant-gas].
- [30] P. B. Blakie, D. Baillie, L. Chomaz, and F. Ferlaino, “Supersolidity in an elongated dipolar condensate,” *Phys. Rev. Research* **2**, 043318 (2020).
- [31] Joseph C. Smith, D. Baillie, and P. B. Blakie, “Supersolidity and crystallization of a dipolar bose gas in an infinite tube,” *Phys. Rev. A* **107**, 033301 (2023).
- [32] J. Sánchez-Baena, C. Politi, F. Maucher, F. Ferlaino, and T. Pohl, “Heating a dipolar quantum fluid into a solid,” *Nature Communications* **14**, 1868 (2023).
- [33] Mingyang Guo, Fabian Böttcher, Jens Hertkorn, Jan-Niklas Schmidt, Matthias Wenzel, Hans Peter Büchler, Tim Langen, and Tilman Pfau, “The low-energy goldstone mode in a trapped dipolar supersolid,” *Nature* **574**, 386–389 (2019).
- [34] L. Tanzi, S. M. Roccuzzo, E. Lucioni, F. Famà, A. Fioretti, C. Gabbanini, G. Modugno, A. Recati, and S. Stringari, “Supersolid symmetry breaking from compressional oscillations in a dipolar quantum gas,” *Nature* **574**, 382–385 (2019).
- [35] G. Natale, R. M. W. van Bijnen, A. Patscheider, D. Petter, M. J. Mark, L. Chomaz, and F. Ferlaino, “Excitation spectrum of a trapped dipolar supersolid and its experimental evidence,” *Phys. Rev. Lett.* **123**, 050402 (2019).
- [36] L. Tanzi, J. G. Maloberti, G. Biagioni, A. Fioretti, C. Gabbanini, and G. Modugno, “Evidence of superfluidity in a dipolar supersolid from nonclassical rotational inertia,” *Science* **371**, 1162–1165 (2021).
- [37] D. Petter, A. Patscheider, G. Natale, M. J. Mark, M. A. Baranov, R. van Bijnen, S. M. Roccuzzo, A. Recati, B. Blakie, D. Baillie, L. Chomaz, and F. Ferlaino, “Bragg scattering of an ultracold dipolar gas across the phase transition from bose-einstein condensate to supersolid in the free-particle regime,” *Phys. Rev. A* **104**, L011302 (2021).
- [38] Giulio Biagioni, Nicolò Antolini, Aitor Alaña, Michele Modugno, Andrea Fioretti, Carlo Gabbanini, Luca Tanzi, and Giovanni Modugno, “Dimensional crossover in the superfluid-supersolid quantum phase transition,” *Phys. Rev. X* **12**, 021019 (2022).
- [39] T. Bland, E. Poli, C. Politi, L. Klaus, M. A. Norcia, F. Ferlaino, L. Santos, and R. N. Bisset, “Two-dimensional supersolid formation in dipolar condensates,” *Phys. Rev. Lett.* **128**, 195302 (2022).
- [40] Matthew A. Norcia, Elena Poli, Claudia Politi, Lauritz Klaus, Thomas Bland, Manfred J. Mark, Luis Santos, Russell N. Bisset, and Francesca Ferlaino, “Can angular oscillations probe superfluidity in dipolar supersolids?” *Phys. Rev. Lett.* **129**, 040403 (2022).
- [41] L. Tanzi, E. Lucioni, F. Famà, J. Catani, A. Fioretti, C. Gabbanini, R. N. Bisset, L. Santos, and G. Modugno, “Observation of a dipolar quantum gas with metastable supersolid properties,” *Phys. Rev. Lett.* **122**, 130405 (2019).
- [42] Fabian Böttcher, Jan-Niklas Schmidt, Matthias Wenzel, Jens Hertkorn, Mingyang Guo, Tim Langen, and Tilman Pfau, “Transient supersolid properties in an array of dipolar quantum droplets,” *Phys. Rev. X* **9**, 011051 (2019).
- [43] L. Chomaz, D. Petter, P. Ilzhöfer, G. Natale, A. Trautmann, C. Politi, G. Durastante, R. M. W. van Bijnen, A. Patscheider, M. Sohmen, M. J. Mark, and F. Ferlaino, “Long-lived and transient supersolid behaviors in dipolar quantum gases,” *Phys. Rev. X* **9**, 021012 (2019).
- [44] Matthew A. Norcia, Claudia Politi, Lauritz Klaus, Elena Poli, Maximilian Sohmen, Manfred J. Mark, Russell N. Bisset, Luis Santos, and Francesca Ferlaino, “Two-dimensional supersolidity in a dipolar quantum gas,” *Nature* **596**, 357–361 (2021).
- [45] A. Filinov, N. V. Prokof’ev, and M. Bonitz, “Berezinskii-kosterlitz-thouless transition in two-dimensional dipole systems,” *Phys. Rev. Lett.* **105**, 070401 (2010).
- [46] Miki Ota and Sandro Stringari, “Second sound in a two-dimensional bose gas: From the weakly to the strongly interacting regime,” *Phys. Rev. A* **97**, 033604 (2018).
- [47] Pedro C. Diniz, Eduardo A. B. Oliveira, Aristeu R. P. Lima, and Emanuel A. L. Henn, “Ground state and collective excitations of a dipolar bose-einstein condensate in a bubble trap,” *Scientific Reports* **10**, 4831 (2020).
- [48] Matteo Ciardi, Fabio Cinti, Giuseppe Pellicane, and Santi Prestipino, “Supersolid phases of bosonic particles in a bubble trap,” *Phys. Rev. Lett.* **132**, 026001 (2024).
- [49] Maria Arazo, Ricardo Mayol, and Montserrat Guilleumas, “Shell-shaped condensates with gravitational sag: contact and dipolar interactions,” *New Journal of Physics* **23**, 113040 (2021).
- [50] M. Nilsson Tengstrand, P. Stürmer, J. Ribbing, and S. M. Reimann, “Toroidal dipolar supersolid with a rotating weak link,” *Phys. Rev. A* **107**, 063316 (2023).
- [51] Luis E. Young-S. and S. K. Adhikari, “Spontaneous dipolar bose-einstein condensation on the surface of a cylinder,” *Phys. Rev. A* **108**, 053323 (2023).
- [52] Marija Šindik, Tomasz Zawislak, Alessio Recati, and Sandro Stringari, “Sound, superfluidity and layer compressibility in a ring dipolar supersolid,” (2023), arXiv:2308.05981 [cond-mat.quant-gas].
- [53] K. Mukherjee, T. Arnone Cardinale, and S. M. Reimann, “Selective rotation and attractive persistent currents in

- anti-dipolar ring supersolids,” (2024), arXiv:2402.19126 [cond-mat.quant-gas].
- [54] Hari Sadhan Ghosh, Soumyadeep Halder, Subrata Das, and Sonjoy Majumder, “Induced supersolidity and hypersonic flow of a dipolar bose-einstein condensate in a rotating bubble trap,” (2024), arXiv:2402.13422 [cond-mat.quant-gas].
- [55] Y. Colombe, E. Knyazchyan, O. Morizot, B. Mercier, V. Lorent, and H. Perrin, “Ultracold atoms confined in rf-induced two-dimensional trapping potentials,” *Europhysics Letters* **67**, 593 (2004).
- [56] Kuei Sun, Karmela Padavić, Frances Yang, Smitha Vishveshwara, and Courtney Lannert, “Static and dynamic properties of shell-shaped condensates,” *Phys. Rev. A* **98**, 013609 (2018).
- [57] Aristeu R. P. Lima and Axel Pelster, “Quantum fluctuations in dipolar bose gases,” *Phys. Rev. A* **84**, 041604 (2011).
- [58] A. R. P. Lima and A. Pelster, “Beyond mean-field low-lying excitations of dipolar bose gases,” *Phys. Rev. A* **86**, 063609 (2012).
- [59] A. Tononi, “Scattering theory and equation of state of a spherical two-dimensional bose gas,” *Phys. Rev. A* **105**, 023324 (2022).
- [60] Jian Zhang and Tin-Lun Ho, “Potential scattering on a spherical surface,” *Journal of Physics B: Atomic, Molecular and Optical Physics* **51**, 115301 (2018).
- [61] Juha Javanainen, Sun Mok Paik, and Sung Mi Yoo, “Persistent currents in a toroidal trap,” *Phys. Rev. A* **58**, 580–583 (1998).
- [62] M. Nilsson Tengstrand, D. Bohlm, R. Sachdeva, J. Bengtsson, and S. M. Reimann, “Persistent currents in toroidal dipolar supersolids,” *Phys. Rev. A* **103**, 013313 (2021).
- [63] Xiao-Fei Zhang, Lin Wen, Lin-Xue Wang, G.-P. Chen, R.-B. Tan, and Hiroki Saito, “Spin-orbit-coupled bose gases with nonlocal rydberg interactions held under a toroidal trap,” *Phys. Rev. A* **105**, 033306 (2022).
- [64] A. Ramanathan, K. C. Wright, S. R. Muniz, M. Zelan, W. T. Hill, C. J. Lobb, K. Helmerson, W. D. Phillips, and G. K. Campbell, “Superflow in a toroidal bose-einstein condensate: An atom circuit with a tunable weak link,” *Phys. Rev. Lett.* **106**, 130401 (2011).
- [65] K. C. Wright, R. B. Blakestad, C. J. Lobb, W. D. Phillips, and G. K. Campbell, “Driving phase slips in a superfluid atom circuit with a rotating weak link,” *Phys. Rev. Lett.* **110**, 025302 (2013).
- [66] K. C. Wright, R. B. Blakestad, C. J. Lobb, W. D. Phillips, and G. K. Campbell, “Threshold for creating excitations in a stirred superfluid ring,” *Phys. Rev. A* **88**, 063633 (2013).
- [67] S. M. Rocuzzo, S. Stringari, and A. Recati, “Supersolid edge and bulk phases of a dipolar quantum gas in a box,” *Phys. Rev. Res.* **4**, 013086 (2022).
- [68] D. Baillie and P. B. Blakie, “Droplet crystal ground states of a dipolar bose gas,” *Phys. Rev. Lett.* **121**, 195301 (2018).
- [69] S. M. Rocuzzo, A. Gallemí, A. Recati, and S. Stringari, “Rotating a supersolid dipolar gas,” *Phys. Rev. Lett.* **124**, 045702 (2020).
- [70] A. J. Leggett, “On the superfluid fraction of an arbitrary many-body system at  $t=0$ ,” *Journal of Statistical Physics* **93**, 927–941 (1998).
- [71] Holger Kadau, Matthias Schmitt, Matthias Wenzel, Clarissa Wink, Thomas Maier, Igor Ferrier-Barbut, and Tilman Pfau, “Observing the rosenweig instability of a quantum ferrofluid,” *Nature* **530**, 194–197 (2016).
- [72] Maximilian Sohmen, Claudia Politi, Lauritz Klaus, Lauriane Chomaz, Manfred J. Mark, Matthew A. Norcia, and Francesca Ferlaino, “Birth, life, and death of a dipolar supersolid,” *Phys. Rev. Lett.* **126**, 233401 (2021).
- [73] Juan Sánchez-Baena, Thomas Pohl, and Fabian Maucher, “Superfluid-supersolid phase transition of elongated dipolar bose-einstein condensates at finite temperatures,” (2024), arXiv:2402.01550 [cond-mat.quant-gas].
-